CLAIRE gamma-ray lens: flight and long distance test results

H.Halloin[a,*], P.von Ballmoos[a], J.Evrard[b], G.K.Skinner[a], M.Hernanz[c], N.Abrosimov[d], P.Bastie[e], B.Hamelin[f], V.Lonjou[a], J.M.Alvarez[c], A.Laurens[b], P.Jean[a], J.Knödlseder[a], R.K.Smither[g], G.Vedrenne[a]

[a]CESR, 9 avenue du Colonel Roche, 31400 Toulouse, France
[b]CNES, 18 Avenue Edouard Belin, 31401 Toulouse, France
[c]IEEC, Edifici Nexus, Gran Capità, 2-4, E-08034 Barcelona, Spain
[d]Institut für Kristallzüchtung, 12489 Berlin, Germany
[e]Laboratoire de Spectrométrie Physique, 38402 Saint Martin d'Hères, France
[f]Institut Laue-Langevin, rue des Martyrs, BP 156, 38042 Grenoble, France
[g]ANL, 9700 South Cass Avenue, Argonne, Illinois 60439, USA

ABSTRACT

CLAIRE is a balloon-borne experiment dedicated to validating the concept of a diffraction gamma-ray lens. This new concept for high energy telescopes is very promising and could significantly increase sensitivity and angular resolution in nuclear astrophysics. CLAIRE's lens consists of 556 Ge-Si crystals, focusing 170 keV gamma-ray photons onto a 3x3 matrix of HPGe detectors, each detector element being only 1.4x1.4x4 cm^3. On June 14 2001, CLAIRE was launched by the French Space Agency (CNES) from its balloon base at Gap in the French Alps and was recovered near the Atlantic ocean (500 km to the west) after about 5 hours at float altitude. Pointing accuracy and gondola stabilisation allowed us to select 1^h12' of "good time intervals" for the data analysis. During this time, 33 diffracted photons have been detected leading to a 3σ detection of the source. Additional measurements made on a ground based 205 meters long test range are also presented. The results of this latter experiment confirm those of the stratospheric flight.

Keywords: Stratospheric Flights, Gamma Ray Spectroscopy, Instrumentation for Nuclear Astrophysics, Crystal Diffraction

1. INTRODUCTION

The study of astrophysical nuclear emission lines provides a unique probe to constrain the physics of the most violent phenomena in the universe. Up to now, the observation of high energy lines (from about 100 keV up to several MeV) makes use of geometrical optics (shadowcasting) or quantum optics (Compton scattering). In both of these systems, the collecting area is less than or equal to the detecting area. As a consequence, increasing the signal results in increasing the background noise and it seems that the present technology faces an impasse where bigger is not necessarily better. Besides, the angular resolution of such an instrument is of the order of 1 deg preventing the precise localisatiion of the γ-ray sources. A γ-ray lens may be a good way to overcome this obstacle : by focusing incoming rays from a large collecting area onto a small detector, this lens not only allows high sensitivities but also permits to locate the source precisely.

2. THE DIFFRACTION LENS AND THE CLAIRE PROJECT

Usually, due to their high energy, γ-ray photons are either incoherently scattered or absorbed by matter and focusing them has thus often been considered impossible.

Nevertheless, γ-ray photons can interact coherently in a crystal lattice provided that the incident angles are very small. We made use of this effect (Bragg diffraction) to develop a γ-ray lens. The small incident angle and the high penetration power of γ-rays led us to choose the so-called Laue geometry (γ-rays are deviated while

*Corresponding author. E-mail : hubert.halloin@cesr.fr, Telephone : (+33) (0)5 61 55 67 44

passing through the crystal). The diffraction of an incoming photon only occurs if θ, the incident angle of the photon with respect to the crystal planes, satisfies the Bragg relation :

$$2d\sin(\theta) = n\lambda \tag{1}$$

where d is the crystal plane spacing, n the reflection order, and λ the wavelength of the γ-ray. Based on this principle, the first γ-ray lens for astrophysics has been built by mounting germanium-silicon crystals in concentric rings (see Fig.1). Each crystal is oriented in order to obtain the correct scattering angle for a given

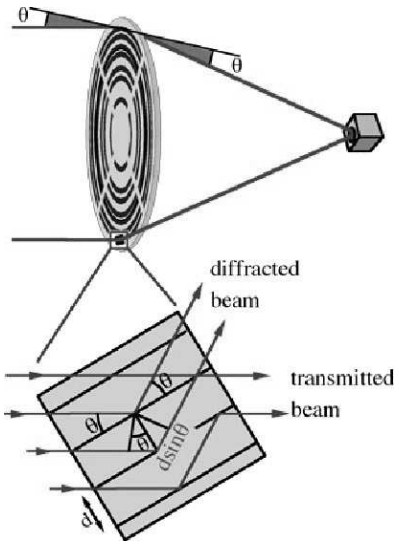

Figure 1. The principle of the gamma-ray lens

incoming energy, from a source at infinity, and thus the lens focuses all the photons to the same focal point. By differentiating the Bragg relation (Eq. (1)), the energy band of a γ-ray lens is seen to be proportional to the square of the diffracted energy :

$$\Delta E \approx \frac{2dE^2\Delta\theta}{hc} \Leftrightarrow \Delta E \approx 40.0 \left(\frac{d}{d_{Ge[111]}}\right)\left(\frac{E}{511keV}\right)^2\left(\frac{\Delta\theta}{1arcmin}\right)\ keV \tag{2}$$

where $\Delta\theta$ is the *mosaic width* of the crystal (typically 1 arcmin), i.e. the angular range over which the crystal reflects monochromatic radiation. $\Delta\theta$ is also a measure of the field of view of the lens. The narrow energy bandpass of the lens is ideally matched to the study of nuclear transitions in the sites of nucleosynthesis (novae, supernovae) and e^+-e^- annihilation.

After having tested the principle of a γ-ray lens (Ref. 1) on the ground and measuring the diffraction efficiency of Ge crystals (Ref. 2), the next step consisted of testing the lens on a astrophysical source : hence the CLAIRE project.

The test of a new instrument can only be done on a well-known source. The incoming flux should also be strong enough to allow a positive detection in approximately a 3 keV broad band and for an exposure time of typically 3 hours. Since no astronomical "standard candle" for γ-ray line emission has been so far discovered, using a section of the continuum emission from the Crab Nebula was an obvious alternative. Thus, while the diffraction lens is dedicated to the observation of nuclear lines, a balloon test flight ironically requires observation of a continuum spectrum. The relatively short focal length of a balloon instrument led us to choose a diffraction energy of 170 keV, resulting in an original 3 m telescope, weighing less than 500 kg (See Fig. 2). For more information about the general design and objectives of CLAIRE, please refer to Ref. 3.

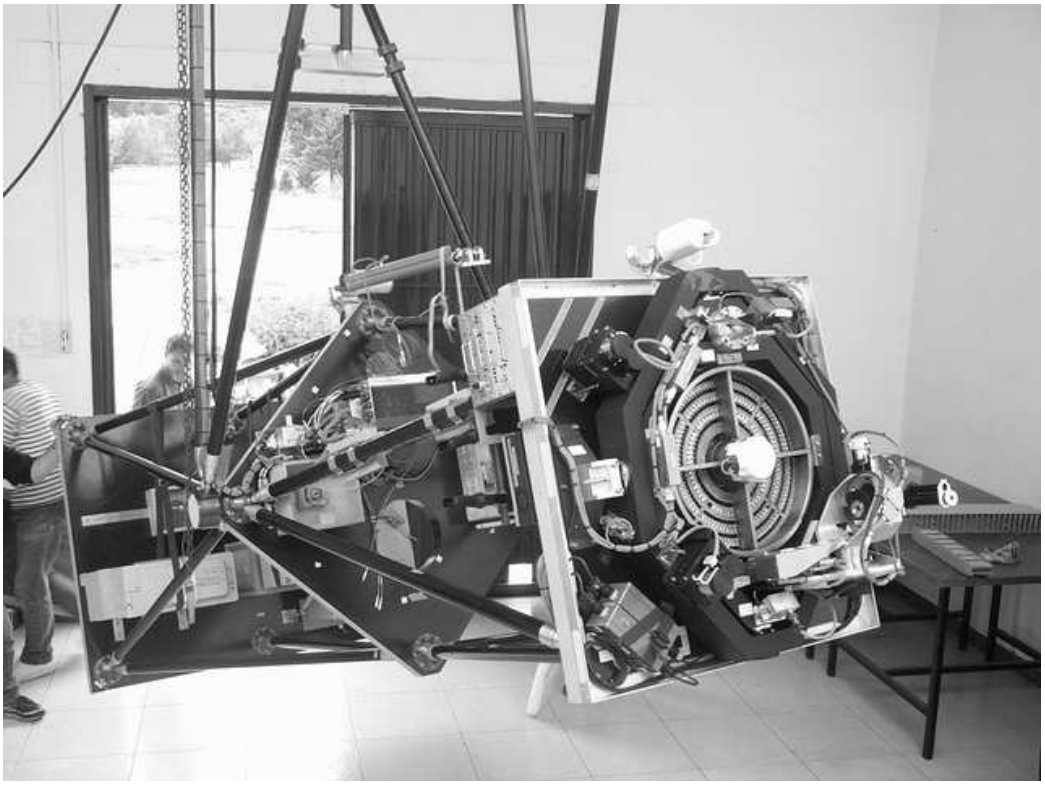

Figure 2. CLAIRE during pointing tests at the launch site.

On June 14 2001, CLAIRE was launched by the French Space Agency (CNES) from its launch site at Gap in the French Alps and landed near the Atlantic coast 500 km west of the launch site. The float altitude was 41 km and lasted about 5 hours.

The lens module, detector package, and pointing systems were built into a purpose designed telescope structure made of composite materials (See Fig. 2). The lens itself is composed of 556 GeSi crystals (511 cm^2 geometrical collecting area) mounted in concentric rings on a titanium frame. The lens and its fine pointing system were held by the upper of three platforms. About 3 meters behind the llens, the lower platform held the detecting system (detector matrix, electronics, collimator, etc.). The γ-ray detector consists of a 3x3 HPGe matrix cooled by liquid nitrogen. Each of the 9 elements is a 1.4x1.4x4 cm^3 n-type coaxial detector with a central hole 0.5 cm diameter x 3.5 cm deep. The pointing system was designed to keep the focal spot on the central detector but it can wander around on the Ge matrix as the primary stabilizer seeks its central position. Background noise in Ge detectors usually dominates over the signal in γ-ray astrophysics and is mainly due to secondary emission induced by cosmic rays (e.g. see Ref. 4). In order to reduce this noise, the matrix was actively shielded by CsI and BGO scintillators. Fig. 3 shows the lens with its fine pointing system (left-hand side) and the Ge-matrix surrounded by the anti-coincidence shield (right-hand side). A detailed description of the fine pointing system and the telescope structure is given in Ref. 5.

3. FINAL FLIGHT RESULTS

A first analysis of CLAIRE's last flight was performed (See Ref. 5) which showed a nominal performance of both pointing and detector systems. The anti-coincidence shield reduced background noise by a factor of 10, resulting in a continuum of about 2.3 10^{-4} cts/s/keV/cm^3 at 170 keV for single events (see Fig. 8(a)). After this background rejection, four lines are significant in the range 50-600 keV : three Ge isomeric transitions (53.4, 139.7 and 198.4 keV) and the e^+-e^- annihilation line (511 keV). Preliminary results showed that the sky and

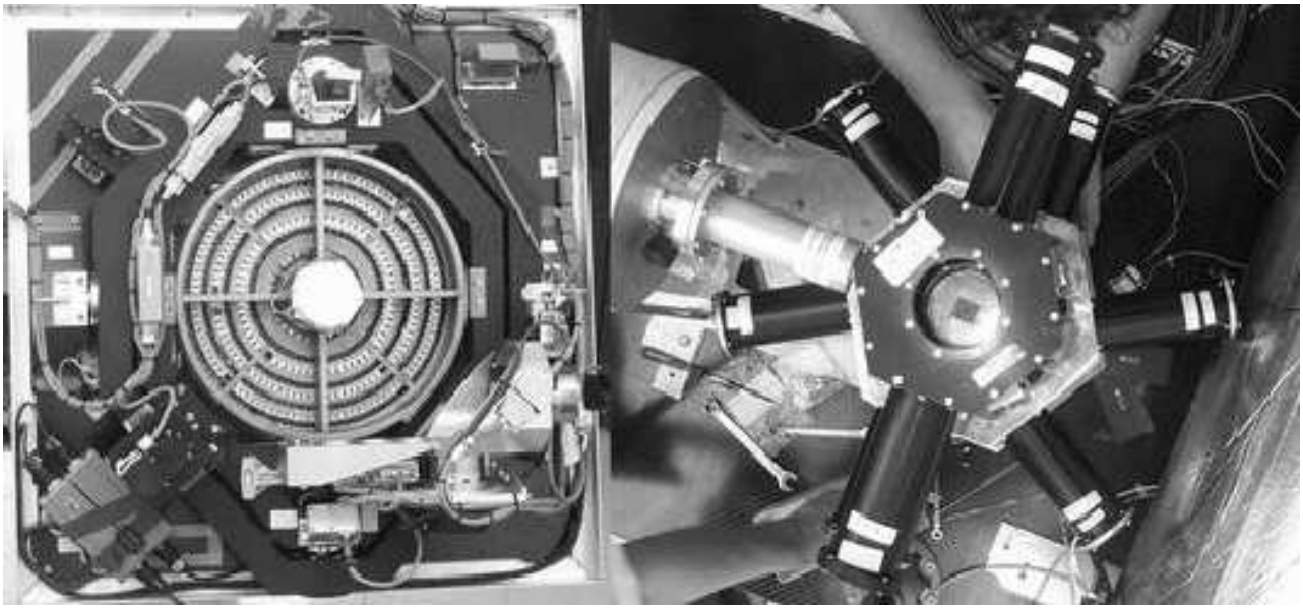

Figure 3. Left : CLAIRE's γ-ray lens (diameter 45 cm on the gimbal mount of the fine pointing system). Right : The 3x3 HP-Ge matrix surrounded by the anti-coincidence shield.

detectors pointing systems achieved very good performances. Nevertheless the reduced spectrum didn't show any evidence of the Crab emission. The reasons which were eventually identified as responsible for this initial absence are explained in the following sections.

3.1. Fine Pointing accuracy

The precise knowledge of the pointing of the lens during the flight is crucial for a good discrimination of events. Actually, as seen by Eq. 1, a variation in the pointing results in different diffracted energies for different crystals and thus a broadening (given by Eq. 2) of the detected peak. This is illustrated by Fig. 4, where some recorded spectra with various pointings of the lens have been plotted. For clarity purpose, successive spectra have been shifted down by a multiple of 1 cts/s/keV. These data were obtained using a 205 m long test range (See Sect. 4). This finite distance explains the position of the diffracted peak at 165 keV (it would be 170 keV for a source at infinity). It appears that the integrated diffracted flux remains roughly constant whereas the FWHM increases. Thus, given the relatively high background noise in γ-ray detectors, an astrophysical signal would rapidly becomes undetectable.

CLAIRE's stabilization and pointing system was developed by the balloon division of CNES. The sun is used as guide star as it is very close to the Crab Nebula around June 14^{th} (about 1 deg). The principle of the fine pointing system is illustrated in Fig. 5.

In order to accurately point the lens at the source (on the ground as well as in flight), a rotating optical telescope with a CCD camera is mounted in the center of the instrument. When looking at an optical source while this telescope is rotated, the image on the CCD describes a circle whose center gives the direction of the rotating axis. This invariant pixel is then used to represent the lens axis. This method provides an alignment accuracy better than 10 arcsec and was used for the tuning of the lens. In order to make this invariant pixel and the zero point of the pointing system correspond during the flight, the sun was simultaneously observed by the central telescope and by the solar sensor. Since the same rotating telescope is used to observe a lamp (on the ground) and the sun, an additional density 6 filter was used for the flight. Unfortunately, the prismatic effect of this filter was not properly measured and an offset effect of about 70 arcsec was recently discovered. Fig. 6 represents the position of the Crab Nebula as seen by the lens during the flight at float altitude corrected for this offset. Simulations making use of the measured pointing and tuning data show that one should consequently

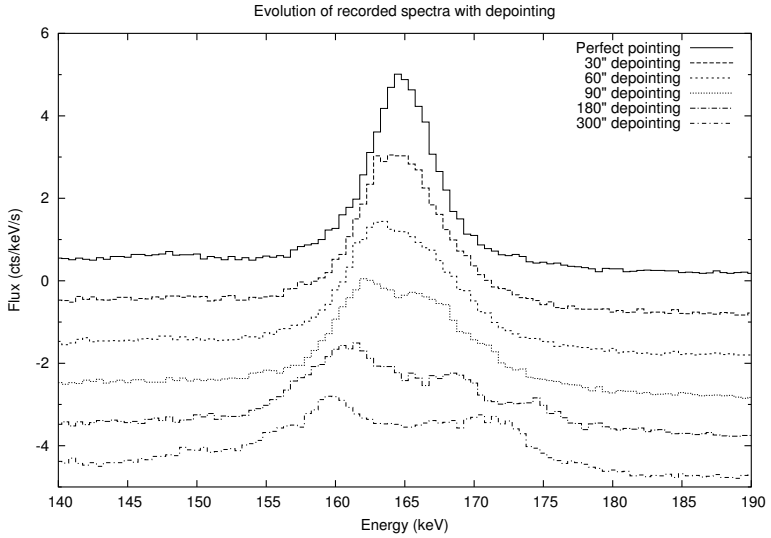

Figure 4. Recorded spectra with a source on and off-axis during ground-based measurements at 205 m. Successive plots have been shifted down for clarity.

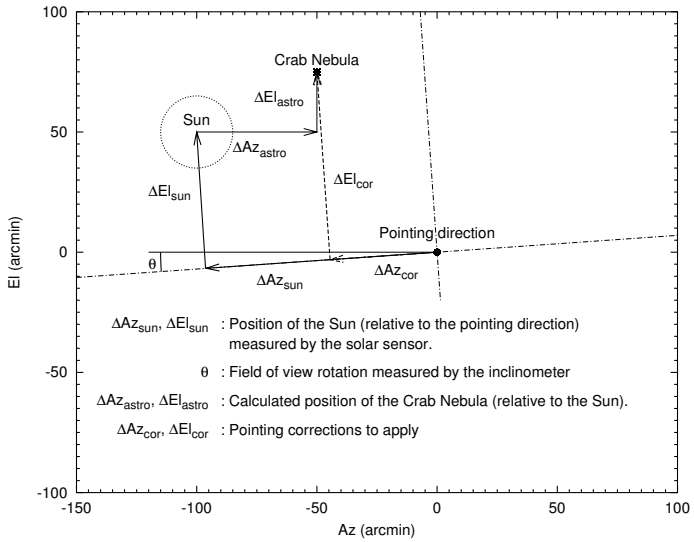

Figure 5. Principle of the fine pointing system. The frame corresponds to the celestial reference, while the dot dashed lines represent the instrument (i.e. CCD camera) axes.

expect the peak at 170 keV to be broadened to 8 keV FWHM.

3.2. Primary pointing accuracy

While, the fine pointing system is dedicated to orientating the lens axis towards the Crab Nebula, the position of the focal spot on the detector matrix depends on a separate, primary, pointing system. This system is designed to stabilize and point the entire telescope in order to keep the detector aligned with the lens. To keep the focal spot on the matrix or on the central detector requires a primary pointing accuracy of $\pm$ 28 and $\pm$ 9 arcminutes, respectively.

As mentioned in Ref. 5, direct use of the fine pointing data did not show any evidence of a peak at 170 keV

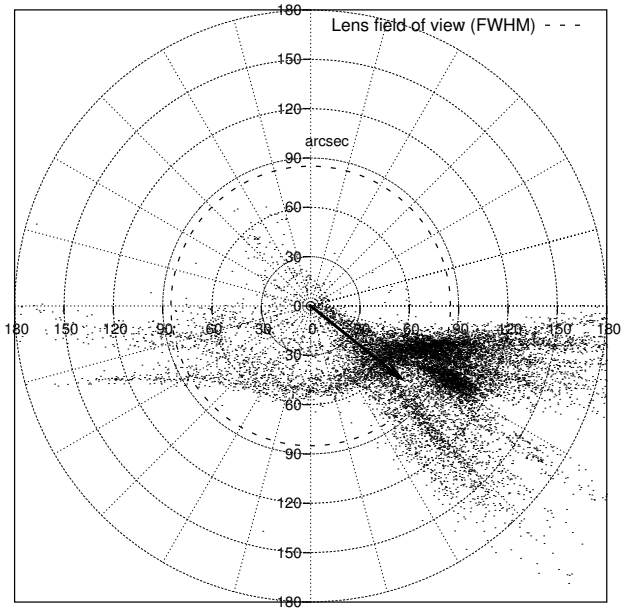

Figure 6. Position of the Crab Nebula as seen by the lens at float altitude. The lens axis is at the center of the graph. The arrow represents the contribution due to the prismatic effect of the solar filter. Each point is the mean value over 1 s.

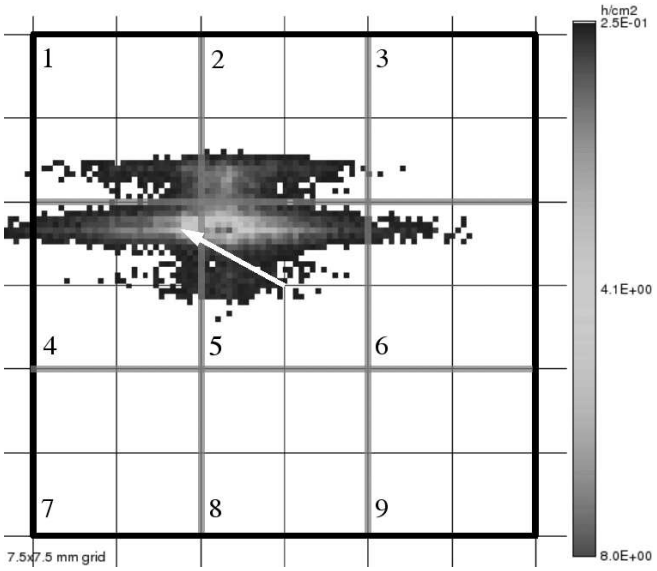

Figure 7. Position of the center of the focal point on the 3x3 Ge matrix during Crab pointing. The arrow shows the displacement of the focal point due to mechanical offsets.

in the flight spectrum. We then suspected a shift of the focal point with respect to the detector. After the reassembling of the telescope structure, comparison of measurements in the orientation typically used during the observations (elevation of about 60 deg) and in the vertical position (used for detector centering) demonstrated that the focal point moved by 4.5 to 6 mm on the vertical axis and between -15 and 15 mm on the horizontal axis.

3.3. Crab detection

As simulation predicts a detected 8 keV FWHM peak at 170 keV, several data analysis were performed with these parameters held fixed while detector offsets were chosen in the mechanicaly admissible area. 30 trials were made with supposed offsets of 5 and 6 mm along the vertical axis and with a 1 mm step scan between -15 and 15 mm along the horizontal axis. The maximum significance during this "fishing expedition" was found with a 3.5 σ (probability of 99.976 %) detection and assuming offsets of +5 mm in the vertical and +10 mm in the horizontal directions. Fig. 7 is a cumulative 2D-histogram of the pointing time on the detector during Crab pointing after correction of these detector offsets. Due to the imperfect stability of the azimuthal axis, the focal point was oscillating from the right (detector 4) to the left (detector 6) with a period of about 170 s. The spectrum corresponding to the maximum significance of the search for the detector offsets is plotted in Fig. 8(b). This spectrum shows a significant excess of about 33 photons at 170 keV with an exposure time of 1^h12. As a comparison, a spectrum of all single events for every detector at float altitude (reference for background) is shown in Fig. 8(a). The higher level of continuum in the background spectrum is mainly due to different background levels in different detectors and to their temporal variability.

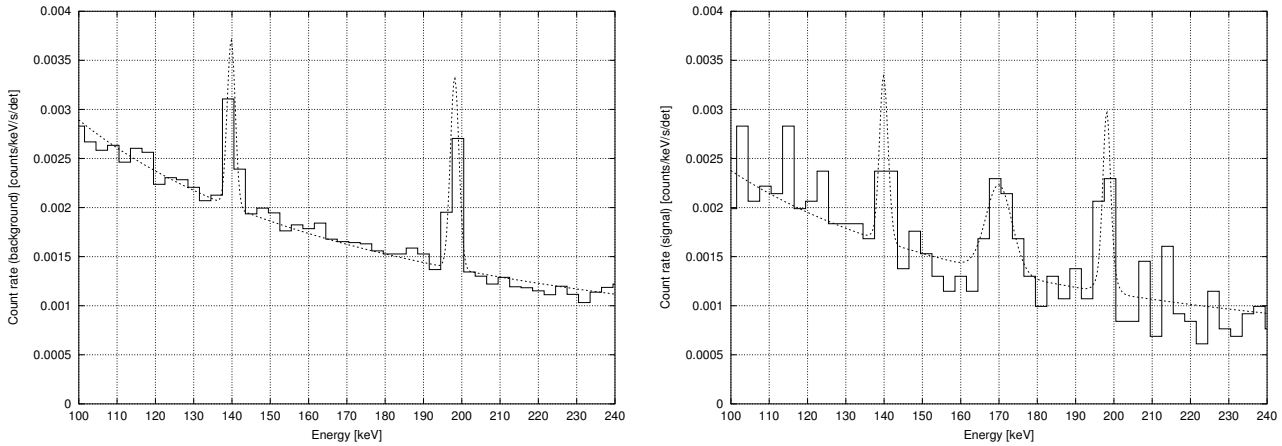

(a) Spectrum for single events at float altitude (background noise spectrum)

(b) Reduced spectrum for single events and good pointing time intervals

Figure 8. Background (left) and pointed (right) spectra.

The number of trials necessary to find this 3.5 σ detection (the search for the detector offsets) should be taken into account. In other words, one should estimate the probability of having a detection greater than 3.5 σ with background noise only and using the same procedure as previously explained (the 30 trials). Actually, the 30 different positions are strongly interdependent since spectra deduced from adjacent positions contain a large number of common events. The probability distribution of "false" detection cannot be easily calculated since it depends (at least) on background noise levels, common good pointing time between different positions, fitting procedures,etc. Nevertheless this probability distribution can be estimated through Monte-Carlo simulations. Knowing the background noise spectrum for each detector during the flight and the respective exposure time for each position of the "fishing expedition", numerous searches on the 30 offsets positions for a positive detection on synthetic data (containing no source !) were performed. For each of these searches the maximum detection is retained and used to estimate the probability of the highest detection be less than n-σ. Fig 9 shows the results of 625 simulations. The probability distribution is very well fitted by a normal distribution with a mean of 2 σ and a standard deviation of 0.47. According to this fit the probability of finding a highest detection less than 3.5 σ while analysing the 30 different data sets of synthetic background is 99.898 %. This figure is then also the corrected detection confidence level. It corresponds to a (single trial) result at the 3 σ level. This also implies that the 30 dependent trials are equivalent to about 4.2 independent trials ($0.99976^{4.2} \approx 0.99898$).

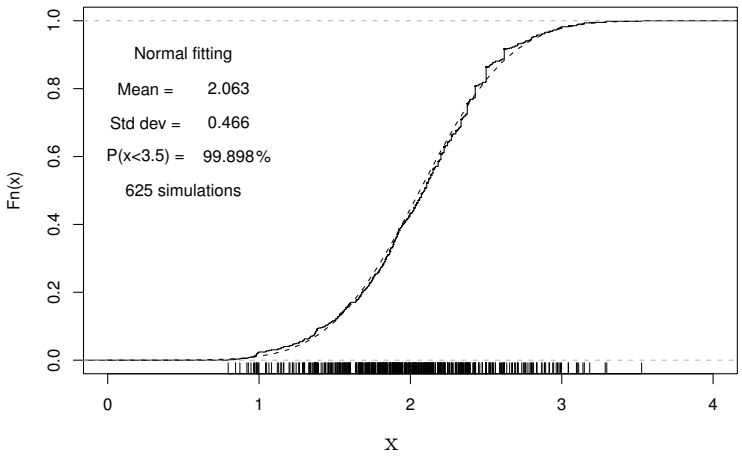

Figure 9. The simulated and fitted probability distribution of false detections in the search for detector offsets. Fn(x) is the probability observed during the simulations with synthetic background that the most significant point among 30 trials is less than x σ.

In the case of an off-axis source, the diffraction peak is broadened but its integral remains roughly constant. Thus, given an estimated FWHM of about 3 keV for a perfect pointed lens (deduced from eq. 2 and the detector resolution), the efficiency of the detectors (≈70 % at 170 keV) and the atmospheric transmission (≈67 % at 170 keV for an altitude of 41 km), the detection of 33 detected photons leads to a peak efficiency of 6.7±1.5 % (i.e 34.2 cm^2 effective area). The efficiency had been estimated using $(4.60 \pm 0.04).10^{-4} \left(\frac{E}{100 \text{ keV}}\right)^{-2.12\pm0.01}$ phot/s/cm^2/keV (see Ref. 6) for the Crab emission , corresponding to $(1.49 \pm 0.02).10^{-4}$ phot/s/cm^2/keV at 170 keV. This efficiency has to be compared with the efficiency deduced from the results of the long distance test (see Sect. 4).

4. LONG DISTANCE TEST

To confirm the results of the flight and to validate the relationship between distance and diffracted energy, a 205 m long test range was set up at an aerodrome at Ordis (near Figueras on the Spanish Mediterranean coast). The X-ray source consisted of a industrial X-ray generator with a 2.5x2.5 mm tungsten target. The voltage and current were set to 250 kV and 1 mA respectively, allowing sufficient X-ray flux at 170 keV after absorption by 205 m of air. The general layout of the experiment is shown in Fig. 10. Analysis of data from this test is still in process but preliminary results are very encouraging.

4.1. Validation of alignment procedures and off-axis response

The alignment method was similar to the one used in the laboratory and in flight : a lamp was mounted just in front of the X-ray source and the lens was pointed in order to make the image of the lamp coincide with the invariant pixel of the rotating camera. The quality of the results obtained by this procedure demonstrates the validity of the invariant pixel as the image of the γ-ray lens axis. Fig. 4 shows spectra obtained with this test range for various pointing offsets with respect to the nominal direction found as above. The broadening of the spectrum with increasing off-axis angle matches very well the prediction of theoretical models.

4.2. Diffracted energy vs distance

According to the Bragg relation (see eq. 1), the diffraction energy increases as the inverse of the incident angle. For the γ-ray lens, this means that the focused energy increases when the distance of the source increases (the

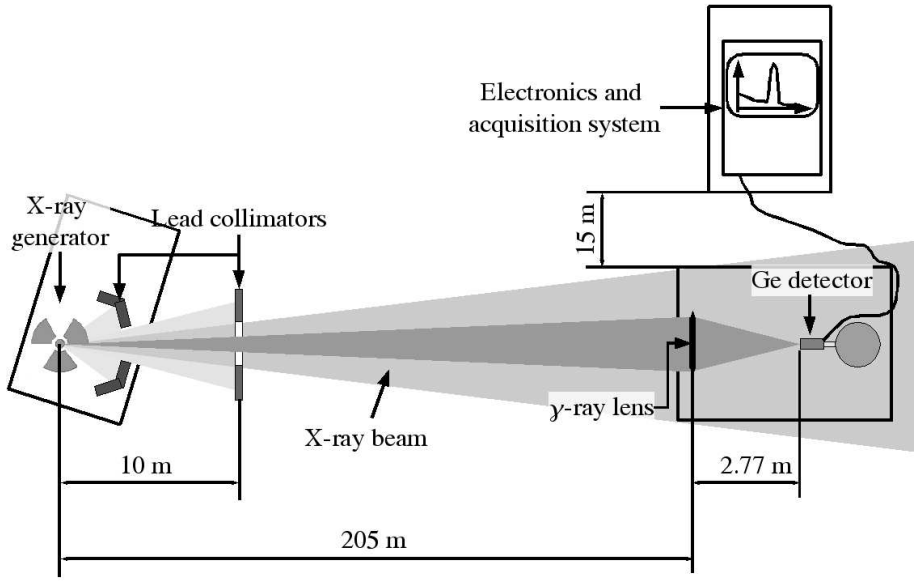

Figure 10. General setting of the long distance test.

lens was tuned to diffract an energy of 170 keV for a source at infinity). The formula giving the relationship between energy and distance is :

$$\begin{aligned} \frac{100\text{ keV}}{E} &= \frac{100\text{ keV}}{E_\infty} + 0.5268\left(\frac{r}{10\text{ cm}}\right)\left(\frac{10\text{ m}}{D}\right)\left(\frac{d}{d_{Ge[111]}}\right) \\ &\approx 0.5882 + 0.3251\left(\frac{10\text{ m}}{D}\right) \quad \text{applied to the CLAIRE } \gamma\text{-ray lens} \end{aligned} \tag{3}$$

where E and E_∞ are the diffracted energies at distance D and at infinity respectively, r is the radius of the ring and d is the distance between diffraction planes. For a γ-ray lens the product $r.d$ must be a constant, otherwise the focal distance for a given energy depends on the ring. According to this formula, the diffracted peak is expected at 165.5 keV for a source at 205 m. After correction for the slope of the incident spectrum, the diffracted peak can be fitted with a Lorentzian centered at 165.2±0.1 keV and a FWHM of 3.9±0.15 keV. The position of the centroid is in very good agreement with theory although slightly lower (possibly due to detector calibration shift but this point is still in investigation). Various measurements demonstrated the validity of this correspondence between distance and diffracted energy (see fig. 11).

4.3. Diffraction efficiency

The width of the peak is wider than expected (3.9 instead of 3 keV) but the following can be responsible, alone or in part, for this broadening :

- The weather was quite windy during the experiment and gusts caused oscillations (i.e off-axis pointing) of the containers and equipment during acquisition.
- When pointing the source with the camera, the air turbulence caused the alignments to be less precise outdoors than those performed in the laboratory or in flight.

However, assuming a "true" width of 3 keV (with the same integrated reflectivity), the peak efficiency is 8.1±0.7 % at 165.5 keV. This result is in good agreement with the peak efficiency deduced from the stratospheric flight

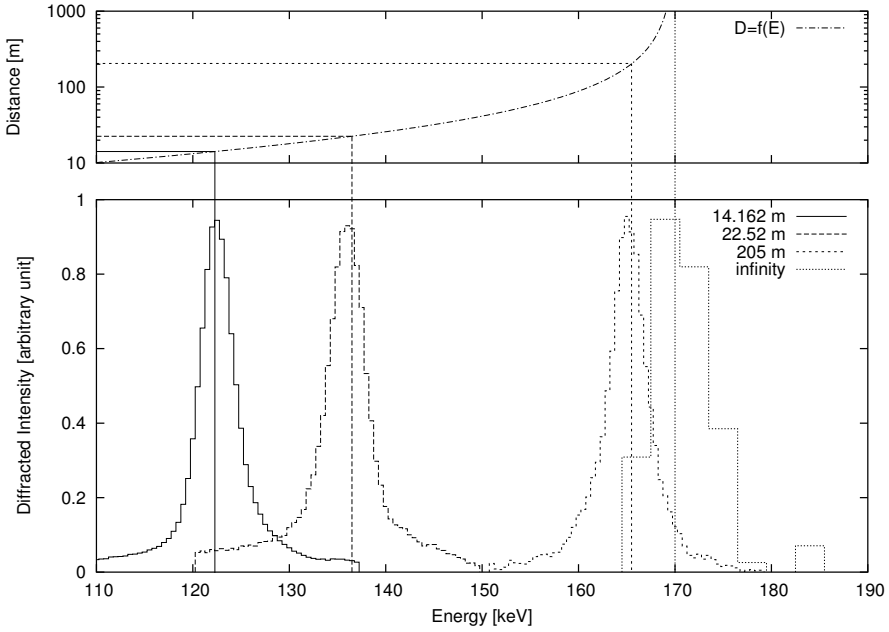

Figure 11. Recorded spectra for various source distances (lower graph). The upper graph represents the distance of the source as a function of diffracted energy. The vertical lines show the theoretical corresponding energies. 14.162 m corresponds to the tuning distance (E_{th}=122.29 keV). The measurement at 22.52 m (E_{th}=136.5 keV) was also done in the laboratory with a partially tuned lens. 205 m is the distance of the generator on the long distance test range (E_{th}=165.5 keV). The peak for an infinite distance is taken from the stratospheric flight (see sect. 3). Slight departures from the theoretical diffracted energy may be due to the shape of the incident spectrum or the calibration drift.

(6.7±1.5 %, see sect. 3). Data obtained during tuning show that some crystals are much more efficient than others (see Ref. 7). Thus, by carefully selecting only the more efficicient crystals, the γ-ray lens efficiency could be increased by a factor of at least 2 or 3.

5. CONCLUSION

CLAIRE's stratospheric flight was the first observation of a astrophysical source with a γ-ray lens. Associated with the ground long distance test, these results validate the theoretical models and demonstrate that the γ-ray lens is a useful tool for nuclear astrophysics.

Ultimately, the crystal diffraction will be used in space where longer exposures, longer focal length and steady pointing will result in outstanding sensitivities (a few 10^{-7}photons$\cdot$s$^{-1}\cdot$cm^{-2}). This project, called MAX, is the subject of another article in these proceedings.[7]

ACKNOWLEDGMENTS

The authors wish to thank the French Space Agency (CNES), which has built the pointing system and operated the flight from the launch to the gondola recovery. This work was supported by the U.S. Department of Energy, Basic Energy Sciences, under contract n° W-31-109-Eng-38.

REFERENCES

1. J. Naya, P. von Ballmoos, R. K. Smither, M. Faiz, P. B. Fernandez, T. Graber, F. Albernhe, and G. Vedrenne, "Experimental results obtained with the positron-annihilation-radiation telescope of the Toulouse-Argonne collaboration," *Nuclear Instruments and Methods in Physics Research A* **373**, pp. 159–164, 1996.

2. A. Kohnle, R. Smither, T. Graber, P. B. Fernandez, and P. von Ballmoos, "Measurement of diffraction efficiencies relevant to crystal lens telescopes," *Nuclear Instruments and Methods in Physics Research A* **416**, pp. 493–504, 1998.
3. P. Laporte, N. Abrosimov, P. Bastie, B. Cordier, G. D. Cocco, J. Evrard, L. Gizzi, B. Hamelin, P. Jean, P. Laurent, P. Paltani, G. K. Skinner, R. K. Smither, and P. von Ballmoos, "Claire - towards the first light for a gamma-ray lens," *Nuclear Instruments and Methods in Physics Research A* **442**, pp. 438–442, 2000.
4. N. Gehrels, "Instrumental background in gamma-ray spectrometers flown in low earth orbit," *Nuclear Instruments and Methods in Physics Research A* **313**, pp. 513–528, 1992.
5. H. Halloin, P. von Ballmoos, J. Evrard, G. K. Skinner, N. Abrosimov, P. Bastie, G. Di Cocco, M. George, B. Hamelin, P. Jean, J. Knodleseder, P. Laporte, C. Badenes, P. Laurent, and R. K. Smither, "Design and flight performance of a crystal diffraction telescope," in *X-Ray and Gamma-Ray Telescopes and Instruments for Astronomy*, J. E. Trümper and H. D. Tananbaum, eds., *Proceedings of SPIE* **4851**, pp. 895–904, 2003.
6. L. M. Bartlett, *High resolution gamma-ray spectroscopy of the Crab.* PhD thesis, University of Maryland, 1994.
7. P. von Ballmoos, H. Halloin, G. K. Skinner, R. K. Smither, N. Paul, J. Abrosimov, M. Alvarez, P. Astier, and P. Bastie, "Max: a gamma-ray lens for nuclear astrophysics," in *Optics for EUV, X-Ray, and Gamma-Ray Astronomy*, O. Citterio and S. L. O'Dell, eds., *Proceedings of SPIE* **5168,this volume**, 2003.